Implosion Physics, Alternative Targets Design and Neutron Effects on Inertial Fusion Systems

G. VELARDE, J.M.PERLADO, J.M. MARTÍNEZ-VAL, E. MÍNGUEZ, M. PIERA, J. SANZ, P. VELARDE, E. ALONSO[&], M. ALONSO, E. DOMINGUEZ, J. G[A] RUBIANO, J.M. GIL, J. G. DEL RIO, D. LODI, L. MALERBA, J. MARIAN[*], P. MARTEL, F. OGANDO, J. PRIETO, S. REYES[*], M. SALVADOR, P. SAUVAN, M. VELARDE

Instituto de Fusión Nuclear (DENIM), E.T.S.I.I., Universidad Politécnica de Madrid, Spain
[*]Present Address: Lawrence Livermore National Laboratory, USA
[&]Present Address: Polytechnique University Zürich, Switzerland
e-mail contact: mperlado@denim.upm.es

Abstract. A new radiation transport code has been coupled with an existing multimaterial fluidynamics code using Adaptive Mesh Refinement (AMR) and its testing is presented, solving ray effect and shadow problems in S_N classical methods. Important advances in atomic physics, opacity calculations and NLTE calculations, participating in significant experiments (LULI/France), have been obtained. Our new 1D target simulation model allows considering the effect of inverse Compton scattering in DT_x targets (x<3%) working in a catalytic regime, showing the effectiveness of such tritium-less targets. Neutron activation of all natural elements in IFE reactors for waste management and that of target debris in NIF-type facilities have been completed. Pulse activation in structural walls is presented with a new modeling. Tritium atmospheric dispersion results indicate large uncertainties in environmental responses and needs to treat the two chemical forms. We recognise recombination barriers (metastable defects) and compute first systematic high-energy displacement cascade analysis in SiC, and radiation damage pulses by atomistic models in metals. Using Molecular Dynamics we explain the experimental evidence of low-temperature amorphization by damage accumulation in SiC.

1. Radiation-Hydrodynamics models for target design

Our Radiation Transport is coupled to the fluid dynamics with a common AMR strategy. However this coupling must be carefully design in order to take advantage of the mesh structure. The ray effect is one of the main drawbacks of the discrete ordinate method. One of the most usual dicretizations of the transport equation is that of diamond differencing, easy to program and calculate, but produces strong ray effects and oscillations. Our work [1, 2] search for new methods to obtain radiation fields with as weak rays as possible. Our new algorithm is oriented to 2D simulations in Cartesian coordinates. Using clean and simple physics and numerical tests [1, 2], relevant to radiation transport and hydrodynamics in Inertial Confinement Fusion (ICF), we have demonstrated the correctness, and availability to be used in sophisticated problems, of our code.

The main point of the algorithms developed consists of supposing an incoming flux distribution. In the simplest case it can be constant over angle and space, or linear. Once a

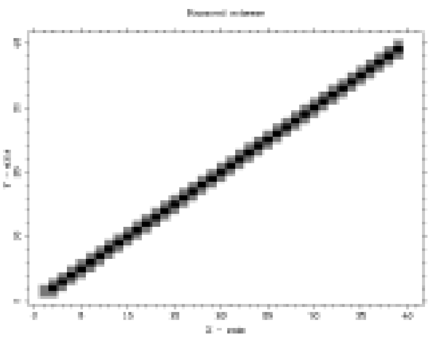

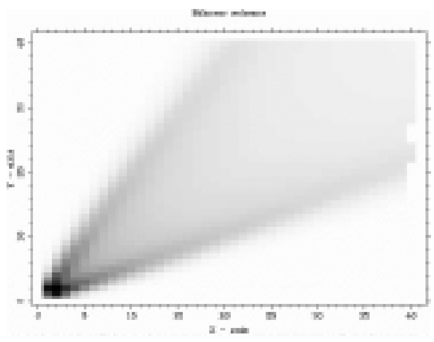

Figure 1.- 2D Radiation Intensities. Ray Effect (left) using S_N vs. our Characteristic model.

base shape is assumed (e.g. constant) that distribution can be defined by a set of scalar parameters (e.g. amplitude). The outgoing distribution will probably not follow the base shape chosen. In order to continue with the calculation on the following cells in the same manner, that outgoing distribution is projected on the base shape set of distributions. This is done in a way such that some functional (like the flux current) is conserved to preserve the shape of the distribution as much as possible. A sample case of a point-like source on the bottom left corner is shown in the Figure 1. Full details of that comparison of the radiation intensity (arbitrary units) between diamond-differencing [S_N (S_2)] and the linear-linear (space and angle) has been published elsewhere [1, 2]. In that figure is shown how using the new algorithm (*right in Figure*) behaves much well under the worst conditions (absence of scattering). The following work is the extension of these methods to 3D geometry and the implementation in a full multigroup transport code. The great advantage of our radiation transport code under AMR is also very remarkable when applied to an isotropic radiation source disk and a disk of high opacity, acting as an obstacle. The shadow effect, which is produced when there are obstacles in the path of the radiation, is clearly reproduced when using these more advanced algorithms [1, 2].

2. Atomic Physics models

Opacity developments have been concentrated in two computer codes: JIMENA and ANALOP [references in 1]. Both have been created to provide frequency-dependent opacities for an average configuration and for detailed configurations. Advanced studies for very high densities are now under development through theoretical studies and by means of experimental work at LULI supported by the European Union HCM Program. These two models have been applied to determine frequency-dependent opacities for plasmas of intermediate and high-Z elements and an extensive comparison with other codes and with experiments has been presented [3]. Using these codes, it has been generated useful analytical opacity formulas for several single elements used in IFE, giving both Rosseland and Planck mean opacities as a function of the temperature and density of the plasma [4]. These formulas are provided as $K_X = a\, T^b.\rho^c$, with X being Rosseland or Planck, T the temperature in eV, ρ the density in $g.cm^{-3}$, and K in $cm^2.g^{-1}$. Constants a, b, c, are given for several elements in Table I that is valid for T's from 50 to 10^4 eV and $\rho = 10^{-3}$ to 10^3 $g.cm^{-3}$. A NLTE atomic kinetic code M3R for the calculation of level population distributions in plasmas was developed in collaboration with the Department of Physics of the University of Nevada. The code solves a set of atomic kinetics rate equations for the plasma for given values of the electron temperature T_e and the electron number density N_e assuming that the

Table I.- Constants for Rosseland and Planck mean opacities.

	Rosseland mean			Planck mean		
Element	a	b	c	a	b	C
Be	18.45	-2.68	0.73	19.51	-2.52	0.76
Cu	21.25	-2.77	0.72	19.36	-2.14	0.42
Al	21.12	-2.80	0.90	20.58	-2.44	0.67
Fe	21.08	-2.77	0.71	18.98	-2.08	0.42
Ge	20.28	-2.60	0.58	18.63	-2.02	0.41
Au	17.17	-2.01	0.33	13.44	-0.85	0.37
Pb	19.83	-1.32	0.45	15.29	-1.34	0.19

electrons can be characterised by a Maxwellian electron distribution function, and also a bi-maxwellian. Either steady state or time-dependent cases can be calculated. Adjacent ground states are linked by electron collisional ionisation (Lotz approximation) and recombination (i.e., three-body recombination), radiative recombination (Seaton´s hydrogenic results) and dielectronic recombination. The excited states of a given ionisation stage are linked to those of the ground states and the next higher ionisation stage, and between themselves by electron collisional excitation (Born approximation) and de-excitation, electron collisional ionisation and recombination, radiative recombination and spontaneous radiative decay. The code has been used for modelling the K_α emission from aluminium ions in non-equilibrium plasmas, and modelling of line emission from Si plasmas produced by femtosecond pulse lasers.

3. The effect of Inverse Compton scattering on the internal breeding of tritium in an ICF target

Tritium will likely be the most significant radiological problem in future *DT* fusion reactors. Therefore, the possibility of a catalytic regime for tritium, where the need of external tritium breeding is avoided, is very important. It was recently shown [references in 1, 5] that a small amount of tritium added to deuterium plasma enables us to trigger ignition at less than 10 keV and internal tritium breeding takes place as the fusion pellet burns up. The main point is the burning temperature, which depends on several parameters, as the initial density of the compressed target when the fusion burst starts. It is also worth pointing out that Inverse Compton scattering can play a very important role in the energy equations of ICF plasma.

To estimate the radiation losses due to inverse Compton effect without fully solving the complicated problem of radiation transport*, a simple model based on the optically thin limit is adopted* [1]**.** The model search for an *equivalent temperature* to be used in the planckian formulation, through a comparison of the real intensities. Although this simplified model is based on the optically thin plasma limit, we verify that for typical parameters (10 g/cm^2, 5000 g/cm^3 and T_e=10 keV) for which the plasma is optically thick, the model also works because the radiation temperature is about equal to the electron temperature. That case yields a value of equivalent T_r equal to the one derived for optically thin up to a factor of $(4/3)^{1/4}$=1.07. Some calculations have been carried out in order to feature the effect of Inverse Compton scattering on the target explosion evolution. For example, a fusion burst started in a target made of DT_x with x=0.0112, and previously compressed up to 5000 g/cm^3 and 10 keV can be cited. If the calculations are done without including Inverse Compton Scattering, the maximum ion temperature is higher than 300 keV and the tritium breeding ratio (final contents to initial load) is 1.75. However, when the Inverse Compton effect is included, the maximum temperature is about 210 keV and the breeding ratio 1.1.

4. Computational modeling of radioactive inventories under IFE irradiation scenarios

Traditionally, activation calculations to model the pulsed mode of inertial fusion energy (IFE) power reactors have used an “equivalent steady state” method. It has been shown, however, that this approach may not yield accurate results for all cases of interest. Our research assess the applicability of a new continuous-pulsed (CP) approach to predict that neutron-induced activation, which has been applied to National Ignition Facility (NIF) and the FSW of HYLIFE-like reactor [6 and references therein]. This model assumes a continuous irradiation period followed by a series of pulses prior to shutdown, and the total fluence and operation time is conserved. The number of those pulses is demonstrated to be short. The Figure 2 shows the effect of increasing the number of pulses in the CP model. The results follow the trends suggested by the analytical study [6]. With only 25 pulses (FSW of HYLIFE-like), the

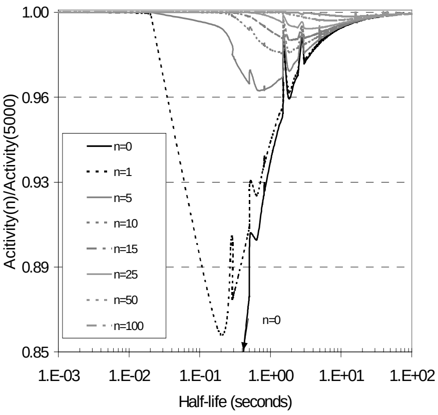

Figure 2. - Ratio of radionuclide activities for different number of pulses, n, prior to Shutdown to long 5000 pulses [6]

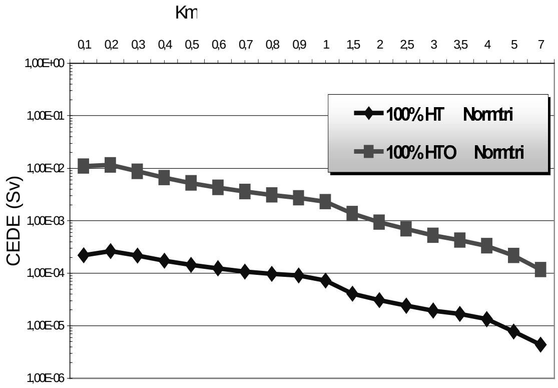

Figure 3.- Effective dose equivalent vs. distance for HT and HTO in normal conditions [7].

nuclides worst treated have an activity ratio of 0.993. With only 50 pulses the error for the activity of any radionuclide is found to be less than 0.35%

In IFE, it is very important to model the activation of target debris. The importance of this radioactivity source, namely for *hohlraum* targets, is still an open question. The S&E characteristics of target materials for IFE have been recently studied, addressing the recycling, waste management, and accident dose characteristics [refs. in 1]. Also, we study the problem of computing the radioactive inventory resulting from the activation of target and near-target materials in NIF-type facilities. A new capability has been included in the inventory code ACAB that considers the irradiation of the target when located in the center of the cavity and irradiation of the material when deposited over the inner surface of the chamber [refs.in 1].

Calculations, using different codes have been performed [references in 1, 7] concluding with very different answer depending on the many parameters that control the consequences. In particular, 100 % release for different reactors, assuming published design points in spite of new claimed conditions, have been reported that show peak values always lower than workers limit, attaining public limit in very short distance (300 m) surrounding the emission. The different behavior of HT and HTO chemical forms is being carefully studied, Figure 3.

5. Radiation Damage of Materials in IFE. Multiscale Modeling approach.

One of the key aspects in Inertial Fusion is the pulse nature of the particle emission. The research has been simply speculating on that effect in the material damage. We are now presenting simulation results on the microscopic understanding of the pulse effect using cascade analysis by Molecular Dynamics (MD) and transport of defects by Kinetic MonteCarlo (KMC) on Cu and Fe metals [8], up to significant doses (*realistic irradiation*), [8]. When the vacancy concentration is represented versus the evolution time and for two different frequencies 10 and 100 Hz, the net effect observed in time is the total accumulation of defects in the structure, in spite of the potential annealing between pulses. However, it can be envisioned that the extension of those numbers to lower frequencies (1Hz) can arrive to an effective annealing between pulses. A rapid recombination between mobile Self-Interstitial Atoms (SIA) and immobile vacancy clusters is a reason, together with a slow break of small vacancy clusters in free vacancies that migrate and shrink SIA clusters or agglomerate with other vacancy clusters. Continuous irradiation at 10^{-4}dpa.s^{-1} is similar to low frequency in Fe.

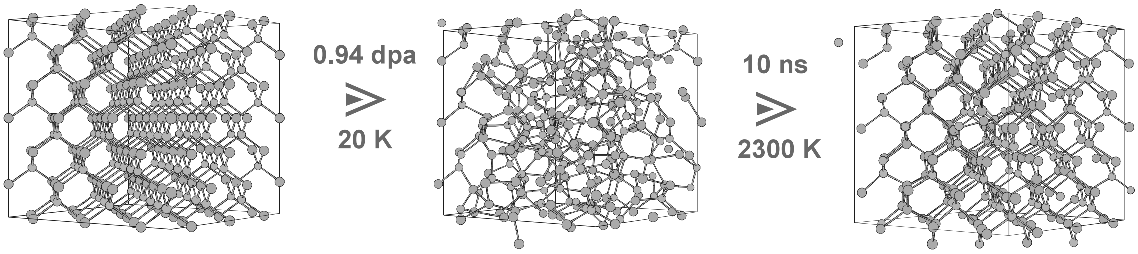

Figure 4. - Crystal Structure of SiC: initial (left); after amorphization coincident in dose with experiments (center); disordered after annealing (right)

However, that situation changes if even lower steady-state irradiation is assumed (10^{-6}dpa.s^{-1}).

We show [9] that in the case of SiC *energy bands* appear, below the classically assumed values of threshold displacement energies, within which displacement is also produced. That modifies for this material the computation of the *dpa*. Our interpretation of such phenomenon is the existence in SiC of *recombination barriers (≈ 1.16 eV)*, which allow the appearance of metastable defects. The upper and lower limits decrease with temperature increases. A first systematic analysis of displacement cascades in SiC have been performed [9, 10], in which our basic results are key to explain most of distinct performance for each sublattice. The irradiation-induced amorphization offers a good possibility to compare our computational results with experiments [11], and proof the relevance of our results in SiC modeling. We used results from 2 MeV electron experiments to induce amorphization in β-SiC at a *critical dose* of 1 dpa for T < ≈250 K. Our critical dose by modeling was 0.94 dpa, and a very good agreement is also in the antisite fraction and the energy per atom. We assure to have reached the amorphous state by checking different physics magnitudes (long range order, short-range order parameters, and pair distribution function). A very important result is the conclusion of a really *disordered* state after annealing of the material.

Acknowledgements
Work funded by the European Union (EU) Commission *keep-in-touch Programme* on Inertial Fusion Energy, EU Mobility, and EU Marie Curie Research Training-Grant, Fusion Programme/ERB-5004-CT97-5002. It has also partially financed by DTN of Spanish Electric Utilities. Areas related to radioactive inventories and materials damage have also been performed under the auspices of the US DoE by LLNL under contract W-7405-Eng-48.

References
[1] G. Velarde et al., Nuclear Instruments and Methods B, accepted for publication (2000)
[2] F. Ogando and P. Velarde, Mathematics and Computation 99, 1772, Senda Ed. (1999)
[3] F.J.D. Serduke et al., J. Quant. Spectroscopy and Radiative Transfer **65** (2000) 527.
[4] E. Minguez et al., Laser and Particle Beams **17** (1999) 1.
[5] J. M. Martínez-Val, S. Eliezer, Z. Henis, and M. Piera, *Nuclear Fusion* **38** (1998) 1651
[6] J. Sanz, P. Yuste, S. Reyes, and J.F. Latkowski, *Efficient modeling for pulsed activation in inertial fusion energy reactors*, Fusion Engineering and Design (2000) In press.
[7] M. Velarde, J. M. Perlado, accepted for Fusion Engineering Design (2001)
[8] E. Alonso, M. Caturla, T. D. de la Rubia, J. Marian, M. Perlado, R. Stoller, J. Nucl. Mater. (2000)
[9] J.M. Perlado, L. Malerba, A. Sánchez-Rubio, T. Díaz de la Rubia, J. Nucl. Mater. **276** (2000) 235
[10] L. Malerba, J.M. Perlado, I. Pastor, T. Díaz de la Rubia, T., *ASTM STP 1405* (2000)
[11] L. Malerba, J.M. Perlado, A. Sánchez-Rubio, I. Pastor, L. Colombo and T. Díaz de la Rubia., J. Nucl. Mater. (2000) In press. L. Malerba, J. M. Perlado, Book of Fabrication and Properties of Ceramics for Fusion Energy and others environ. American Ceramics Society Pub. (2000)